IEEE Access
Multidisciplinary ⋮ Rapid Review ⋮ Open Access Journal

Received December 23, 2021, accepted January 12, 2022, date of publication February 9, 2022, date of current version February 16, 2022.

Digital Object Identifier 10.1109/ACCESS.2022.3150331

Security Assessment for the Islanding Transition of Microgrids

PATRY J. COLORADO[1], VINICIUS P. SUPPIONI[2], ALFEU J. SGUAREZI FILHO[2], (Senior Member, IEEE), MAURÍCIO B. C. SALLES[1], (Member, IEEE), AND AHDA P. GRILO-PAVANI[2], (Senior Member, IEEE)

[1]Laboratory of Advanced Electric Grids—LGrid, Polytechnic School, University of São Paulo (USP), São Paulo 05508-010, Brazil
[2]Center for Engineering, Modeling and Applied Social Sciences (CECS), Federal University of ABC (UFABC), Santo André, São Paulo 09210-580, Brazil

Corresponding author: Patry J. Colorado (patry.colorado@usp.br)

This work was supported in part by the Coordenação de Aperfeiçoamento de Pessoal de Nível Superior Brasil (CAPES) Finance Code 001, in part by the University of São Paulo, in part by the Project FAPESP 2018/20104-9, and in part by Project CNPq 438365/2018-6.

ABSTRACT Grid-connected microgrids pose a risk of unsuccessful transition to islanded operation due to unintentional islanding. The success of this transition is influenced by different factors, such as the operating point, the controls, and the islanding detection scheme. This work proposes a methodology to access the probability of a successful transition of a microgrid from grid-connected to islanded mode. The methodology is based on Monte Carlo simulations using probabilistic curves for representing the operating point of the distributed energy resources, loads, and storage devices. The method is validated by performing an analysis of the islanding transition of a hybrid RE-storage-diesel microgrid, either employing a Battery Energy Storage System (BESS) or Flywheel Energy Storage (FES). The use of the proposed method allowed an assessment of the influence of the capacity of the storage units on the success of the islanding transition.

INDEX TERMS Microgrid, islanding transition, distributed energy resources.

I. INTRODUCTION

Microgrids comprise multiple distributed energy resources, especially renewable, and employ controls and energy storage devices to keep their operation efficient and stable in both possible operating modes, islanded or grid connected. In addition, the deployment of microgrids allows not only the efficient integration of distributed energy resources, but it is also considered an effective solution for enhancing the grid resilience, due to their ability of operating in islanded mode when of the connection to the main grid is lost [1]. However, to reach this resilience, the microgrid must remain stable during the different disturbances that these grids are subjected. Among the possible disturbances, the nonintentional islanding is considered one of the most difficult disturbance to deal with, mainly because it requires the identification of the change in the operating mode, grid-connected to islanded, and a change in the controls of the Distributed Generation (DG) units [2], [3].

The associate editor coordinating the review of this manuscript and approving it for publication was Bin Zhou.

Different controls can be applied to improve the microgrid stability during the transition from grid-connected to islanded operation mode due to an unintentional islanding occurrence. In a microgrid, the frequency behavior after disturbance is critical due to the low inertia, since renewable sources are connected by converters, which do not have intrinsic inertia. If the microgrid does not have promptly available power to supply the loads, a load shedding scheme should be performed to ensure the islanded operation. These schemes basically monitor the microgrid frequency and shed the loads to keep the frequency. However, due to the low inertia of microgrids, the microgrid can lose stability during the islanding transition, even with enough power due to the delay in changing the DG control mode [4].

For the wind generators, synthetic inertia can be used to support frequency during the transition to islanded mode. Besides, there are controls proposed in the literature to improve the voltage and frequency variations during this transition. A fast response of these controls depends on the identification of the islanding condition. Once the islanding condition is identified, a signal is sent to a centralized or a

distributed control scheme of the microgrid, which changes the DG units control objectives to provide both voltage and frequency support to the islanded microgrid (*Vf mode*). The voltage and frequency variations, as well as the microgrid stability, depends on the load-generation unbalance and on the controls used in the microgrid [2].

Considering that one of the advantages of microgrids is supplying the needs of local consumers in a continuous and safe way, load shedding is being considered as the last alternative to avoid instability. Several aspects must be accounted for to enable a successful transition, for example, the low inertia and intermittency, characteristics of renewable energy sources, which can compromise the stability of the microgrid during the islanding transition.

Thus, the islanding transition may fail due to different factors or a combination of these factors. A typical issue for the transition is the performance of the islanding detection scheme. Delays in identifying the islanding condition may result in maintaining the operation without changing the controls of DG units. In this case, any variation of the load will result in large excursions of voltage and frequency. The low inertia of these systems is also an issue and results in high rate of frequency change when the power imbalance is high at the islanding occurrence. Additionally, issues related to the control settings may also impact in the performance of the microgrid in the transition to islanded operation.

Different studies have shown that the deployment of microgrids improves the resilience of power distribution systems, as pointed out by simulations studies presented in [5]–[11]. In [5], it is described a methodology to quantify the economic and resiliency benefit provided by renewable energy in a hybrid RE-storage-diesel microgrid, focusing on quantifying the outage survivability associated with renewable system. References [6]–[10] show that microgrids can keep supplying the loads during an interruption from the utility distribution grid and propose different strategies to extend load capacity of the microgrid in the islanded mode. However, the approaches do not evaluate the transient behavior of the microgrid during the islanding transition.

In [11], it is proposed a method to increase reliability of supply for distribution networks during an emergency in the power system by intentionally separating parts of the distribution system from the main grid to avoid the collapse of the complete system. The paper proposes an Islanding Security Region (ISR) to provide security assessment of islanding operation, including grid code requirements as criteria for successful islanding transition assessment. Using the proposed method, it is possible to determine, by comparing the system operating state with the ISR, whether or not the system could be successfully islanded. The method can be used by the system operator for planed actions, that is, for intentional islanding. However, the method cannot be used for the assessment of unintentional islanding transition. In these cases, the system operating state is uncertain, especially considering the high rate of renewables connected as DG.

It is possible to find in the literature papers that propose methods to improve, or analyze, the success of the islanding transition for a given part of distribution system supplied by DG or for a microgrid [2], [3], [6], [7], [9]. Most of them propose methods to improve the transition or analyzes the main aspects that impacts the transition and performs the tests for specific operating conditions. It can also be found papers that computes reliability indexes based on the failure rates of the microgrid components, but that do not comprise the probability of successful transition to a new operating mode considering the operating conditions.

In this context, the contribution of this paper is the assessment of the successful rate of unintentional islanding transitions of a microgrid. The proposed methodology calculates the probability of success of the islanding transition. It allows modeling the main factors that influence the stability of the microgrid, such as the controls used in the generation units, the power exchange prior to islanding, and the schemes used to detect the islanding condition. The method is based on Monte Carlo Simulation (MCS), and it is validated considering a hybrid RE-storage-diesel microgrid, originally composed of a wind generator and a synchronous generator. As energy storage systems can be used to increase the successful rate, a Battery Energy Storage System (BESS) is connected to evaluate the impact on the islanding transition, as well as a Flywheel Energy Storage (FES).

The remaining of this paper is organized as follows: Section II briefly introduces the nonintentional islanding of microgrids; the proposed methodology is presented in Section III; the system is modeled in Section IV; Section V presents the simulation results; discussions are addressed in Section VI. And finally, section VII presents the conclusions.

II. UNINTENTIONAL ISLANDING OF MICROGRIDS

A microgrid is stable if, after being subjected to a disturbance, all variables return to a steady-state value that satisfies the operational restrictions, without the involuntary occurrence of load shedding [12], [13]. For a microgrid, the nonintentional islanding is considered one of the most difficult disturbances to deal with, mainly because it can occur in adverse operating conditions for the controls to restore frequency and voltage.

In the grid-connected mode, the utility grid is responsible for imposing the voltage and frequency of the microgrid. In this condition, stability depends on the characteristics of the connection point and on the behavior of the individual components connected to the microgrid [4]. In the islanded mode, the control of the frequency and voltage is performed by the resources present in the microgrid and to maintaining a stable operation can be more challenging due to the high penetration of renewable generation; high uncertainty in the system; low inertia; higher R / X ratio of the feeders; low short circuit capacity; less available power; and unbalanced three-phase loads [4], [14]–[16].

Assuming that the utility grid does not demand a fixed active or reactive power injection at the Point of Common

Coupling (PCC) during the microgrid connected operation, typically, distributed synchronous generators operate with constant power factor and constant active power (*PQ mode*) and wind generators with constant power factor and the active power as a function of wind speed [17]–[19]. In an islanding event, the control mode of the excitation system of synchronous generators is changed to maintain the system voltage, as well as the speed regulator must be changed to maintain the system frequency (*Vf mode*). The wind generation, in turn, can contribute to the system's voltage control and temporarily to the frequency support, using synthetic inertia control [17], [18], [20]. After the islanding occurrence, the new operating mode should be identified, then a signal is sent to change the controls of the DG units to support the grid frequency and voltage. In this process, variations in voltage and frequency depend on the operating condition of the network at the instant of islanding; the disturbance that led to the formation of the island; the islanding detection time, and the alteration of the controls of the DG units responsible for supplying the loads [21].

As a result, this transition can result in large variations in voltage and frequency, which are related to the unbalance between the active and reactive powers generated and consumed at the instant of the islanding occurrence. Thus, the greater the imbalances of the active and reactive powers, the faster changes in the control mode must be implemented. Control strategies can be used in microgrids for smooth transfer from grid-connected to islanded operation [22], [23], which have an influence on its stability. However, the effectivity of these controls also depends on the operation point and the islanding detection time. For example, in [24], it is possible to verify that for some operating conditions, the voltage can violate the lower limit during an islanding transition.

The islanding detection time also influences the successful rate in islanding transitions and depends on the technique employed. Islanding detection techniques can be classified into two main groups: remote or local techniques. Local techniques are classified into passive, active and hybrid techniques. Each method has its advantages and disadvantages, depending on their viability [25]. The detection time can be detrimental to islanding transition when methods based on local measurements are employed and, as consequence, they should be considered in the assessment of the islanding transition.

The remote techniques are efficient and reliable in detecting the operating condition and can be used both to detect the occurrence of islanding and to detect the reconnection of the islanded network to the utility grid. These techniques are based on the communication between the control and protection devices of the electric network and, thus, they detect the operating condition using the information of the state of the switching devices.

Remote techniques can detect islanding quickly, however, they result in high complexity and high installation costs [26]. In addition, currently, most distribution networks do not have a communication system, thus, to not limit the islanded operation of microgrids, techniques that do not depend on communication systems for island detection should be considered in the planning of microgrids.

Local island techniques are based on measurements of voltage, frequency, harmonics, etc., at the terminals of the DG units. These techniques are divided into passive and active. The local active techniques are based on response of the network after the insertion of small disturbances, which is different if the network is islanded or connected. In this way, a small disturbance is introduced into the network whenever it is necessary to check the status of the network. Typically, the range of these disturbances is milliseconds [27].

The local passive techniques are based on the behavior of voltage and frequency signals. The changes in these signals occur due to the unbalance between the power generated by the DG and the power consumed by the loads of the islanded network at the islanding occurrence. These techniques are considered the first option among the techniques for islanding detection, as they employ local schemes usually available, as relays [28]–[32], or can be easily implemented in controller [33].

Techniques that use frequency or voltage relays are practical since the relays are easily obtained on the market at a low cost [28]–[32]. Additionally, in the literature, it is possible to find efficient schemes employing different techniques to detect the islanding. In [34], an intelligent islanding detection method is proposed based on intrinsic mode function feature-based grey wolf optimized artificial neural network. Both ensemble learning and canonical methods are considered for the islanding detection technique of synchronous machine-based distributed generation in [35]. Kalman filter is used to extract and filter the harmonic contents of the voltage signal at DG terminals to identify the islanding operation in [36]. A passive islanding detection scheme using variational mode decomposition-based mode singular entropy for integrated microgrids in [37].

However, passive techniques may fail when the differences between generation and demand are small at the moment of islanding, in these conditions the voltage and frequency variations may not be sufficient to reach the values that sensitize the relays [38], [39].

Hybrid techniques, which consists of using passive and active techniques can compensate the Non-Detection Zone (ZND) of passive techniques and inject less disturbances into the grid, compared to the active techniques [40], [41]. For example, methods proposed in [40], [41] are capable of detecting the islanding or reconnection condition of the microgrid using voltage and frequency measurements. In situations where the variations in voltage and frequency are not sufficient to guarantee the islanded condition, a disturbance in the Synchronous Generator (SG) reference power is injected into the network, using variations in voltage and frequency to identify the operating status of the network. As a result, hybrid techniques for islanding detection present a high potential to enable a suitable operation of microgrids.

Considering all factors discussed, after the islanding occurrence the criteria for assessing if the procedure were successful should include checking if the system response complies with the grid code requirements and the mandatory frequency and voltage tripping. Thus, in view of the great variety of controls and operating conditions involved in the islanding transition, a methodology to access the successful rate of this procedure is presented in the next section.

III. PROPOSED METHODOLOGY

As discussed in the previous sections, the success of the islanding transition highly depends on the performance of the controls applied to regulate frequency and voltage. However, the effectivity of these controls is associated to the operating point, which is a combination of load and generation. Thus, to estimate the probability of the success of the islanding transition of a microgrid, it is necessary to consider all possible combination of operating conditions, which requires modeling the elements that have a stochastic behavior. These elements are loads, solar and wind generation, and BESS. In the case of the BESS, the state of charge should be considered since it represents the energy that the BESS can inject into the grid to ensure a successful transition.

In this sense, a methodology is presented for computing the probability of successful island transition. The methodology is based on MCS, performed using the operating conditions given by the probabilistic distribution functions to estimate load, generation, and state of charge of BESS [42]. The MCS is a statistical method that randomly assigns values to the input variables of the system according to their distribution function. The MCS is one of the main alternatives to assess performance of energy systems considering uncertainty of renewable energy source. The flowchart shown in Fig. 1 presents the procedure to calculate the probability of a successful islanding transition.

As one can see, the first step of Fig. 1 consists of obtaining probabilistic distribution curves for generation, load and State of Charge (SoC) of the BESS in the microgrid. Then, based on these distribution functions, samples of generation, load, and SoC are generated, which are used as input of the microgrid to simulate an islanding occurrence. The system response is then used to check the criteria for islanding assessment, according to the grid code. If the voltage and frequency respect the grid code requirements, the islanding transitions was successful, if not, the islanding transition failed. Following, the successful islanding transition probability is estimated by using:

$$E(X) = \frac{1}{N}\sum_{k=1}^{N} X_k \tag{1}$$

where E (X) is the value that is being estimated. In this case the probability of success of islanding;X_k represents the result for the k-th simulation, with "1" for the successful case and "0" for the failed transition; and N is the total number of simulations.

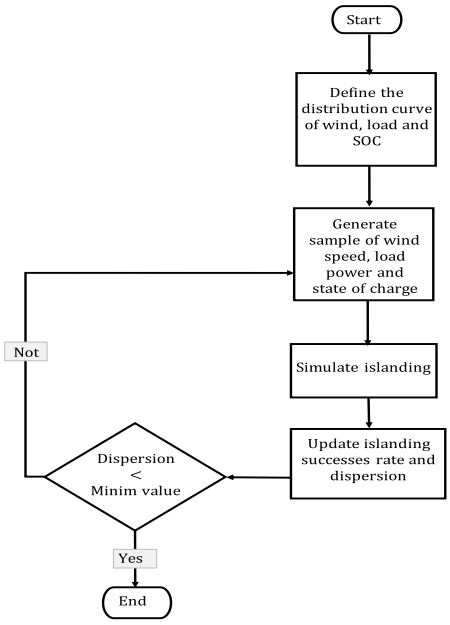

FIGURE 1. Flowchart of the proposed methodology.

The convergence of the system is verified by the dispersion coefficient, β, which is related to the homogeneity of the data of the evaluated system. Thus, the dispersion coefficient, β, will be responsible for indicating that the system has achieved the required minimum reliability. The dispersion coefficient is calculated as follows:

$$\beta = \frac{\sigma[E\,(X)]}{E\,(X)}.100\% \tag{2}$$

The standard deviation, σ, is the square root of the variance, which is used as the data dispersion indicator with respect to the mean arithmetic sample.

Therefore, the value of $\sigma[E(X)]$, given by:

$$\sigma[E(X)] = \frac{\sigma\,(X)}{\sqrt{N}} \tag{3}$$

And σ (X) is calculated by:

$$\sigma(X) = \sqrt{\frac{1}{N-1}\left[\sum_{k=1}^{N} X_k^2 - NE(X)^2\right]} \tag{4}$$

The value of the dispersion coefficient, β, indicates the convergence of the method. A reference value in the range of 2% is normally used, therefore, the simulations reach the convergence when a value lower than this is reached, otherwise, the simulations must continue [42].

A. PROBABILISTIC LOAD DISTRIBUTION MODEL

The loads in distribution networks, due to their different composition and variations, are difficult to represent and the use of a simple Gaussian distribution isn't sufficient for this purpose [43]. Several works that use probabilistic distribution functions to reproduce the load variation can be found in the literature, such as: normal logarithmic in [44],

beta in [45], [46], Weibull [47], and a grouping of various functions in [48].

However, these representations are not comprehensive enough to represent all types of loads. In this sense, the Mixed Gaussian Distribution Method (GMM) has been used for this purpose and has the advantage of representing a wide variability of loads, it is composed of a convex mixture of several normal distributions with their respective means and variances. However, one of its drawbacks is the parametric estimate of the weight, mean and variance of the Gaussian mixture. Usually, the Expectation Maximization (EM) algorithm is used to calculate the parameters of this distribution [49], its function is to find the maximum probability of the parameters in a given set of an underlying distribution, when the data contains missing or incomplete values. So, in this paper it is used the GMM [50], which is represented by:

$$f\left(z \mid \gamma\right) = \sum_{i=1}^{M_c} \omega_i f\left(z \mid \mu_i, \sum_i\right) \tag{5}$$

Therefore, we can say that for each probability distribution "f" there is a mixed component, which, in turn, presents an associated probability ω_{i} being it the weight of the mixture. Where, MC represents the number of mixed components and ω_{i} represents the weight of the i-th mixed component, subject to $\omega_i > 0$ e $\sum_{i=1}^{M_c} \omega_i = 1$. γ is selected from the parameter set $\Gamma = \left\{\gamma : \gamma = \left\{\omega_i, \mu_i, \sum_i\right\}_{i=1}^{M_c}\right\}$. Therefore, for each density component that belong to a random variable gaussian function d-dimensional z, with a mean vector μ_i and covariance matrix $\sum_i$, the density function of each mixing component $f\left(z \mid \mu_i, \sum_i\right)$ is a normal distribution given by:

$$f\left(z \mid \mu_i, \sum_i\right) = \frac{1}{(2\pi)^{d/2} det(\sum_i)^{1/2}} \times e^{\left(-\frac{1}{2}(z-\mu_i)^T \sum_i^{-1}(z-\mu_i)\right)} \tag{6}$$

In a microgrid, load measurements are commonly available. These measurements can be used in an algorithm, as presented in [49] to calculate the parameters of the distribution function.

The system load probability distribution, presented in Fig. 2, was generated using the aforementioned procedure. It is observed that the load distribution of the system does not follow any known distribution function which cannot be represented by a simple distribution function.

B. PROBABILISTIC WIND DISTRIBUTION MODEL

Considering that the Weibull distribution function is the most used probabilistic distribution function to describe the wind distribution [51], it is the one adopted to represent the wind distribution in the work.

$$F_w\left(v\right) = \left(\frac{k}{c}\right)\left(\frac{v}{c}\right)^{k-1} e^{-(v/c)^{\kappa}} \tag{7}$$

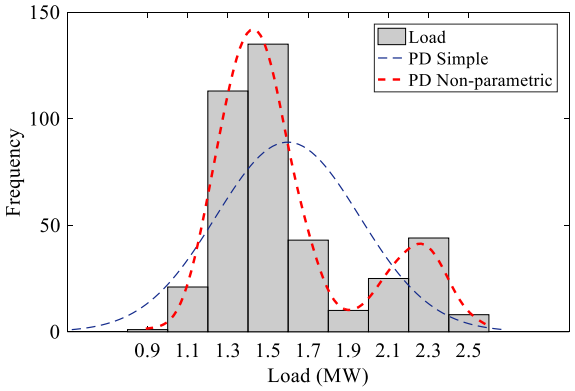

FIGURE 2. Probabilistic load distribution.

where, "v" is the wind speed in m/s, "c" the scale parameter in m/s and "k" the shape parameter (without dimension). Data of wind distribution is commonly available for sites with wind turbines installed, so this data can be used for modeling the distribution function of the wind in the microgrid.

C. PROBABILISTIC DISTRIBUTION MODEL OF THE STATE OF CHARGE OF THE BATTERY

In order to generate random samples of SoC, the multivariate normal distribution was used, it is composed of two parameters a covariance matrix Σ, and a mean vector μ that are analogous to the mean and variance parameters of a univariate normal distribution [52], [53].

The Probability Density Function (PDF) of the d-dimensional multivariate normal distribution is:

$$\begin{aligned} Y &= f\left(x, \mu, \sum\right) \\ &= \frac{1}{\sqrt{\left|\sum\right|(2\pi)^d}} exp\left(-\frac{1}{2}(x-\mu)\sum^{-1}(x-\mu)^*\right) \end{aligned} \tag{8}$$

where μ and x are 1-by-d vectors, and Σ is a d-by-d symmetric, positive definite matrix. Thus, the multivariate normal Cumulative Distribution Function (CDF) calculated at x is the probability that a random vector v, distributed as multivariate normal, lies within the semi-infinite rectangle with upper limits defined by x:

$$Pr\left\{v\left(1\right) \le x\left(1\right), v\left(2\right) \le x\left(2\right), \ldots, v\left(d\right) \le x\left(d\right)\right\} \tag{9}$$

Thus, this distribution function should represent the SoC of the BESS installed at the microgrid. It is important to have an estimation of the storage systems capability to provide frequency support during the islanding transition of a microgrid.

IV. MODELING THE MICROGRID

The proposed methodology is applied in the system presented in Fig. 3.In this system, the microgrid is illustrated in the area highlighted by the dotted line. The microgrid consists of a distributed synchronous generator (DG1), a wind generator (DG2), load and two possible storage systems, a flywheel

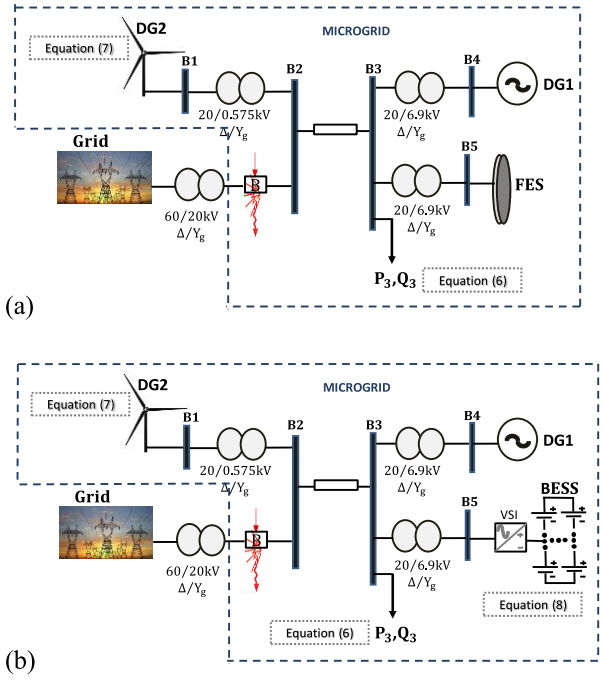

FIGURE 3. Test distribution system.

storage system (FES), considered in the configuration presented in Fig. 3 (a), and a Battery Energy Storage System (BESS), presented in Fig. 3 (b). DG1 presents a nominal power of 3.3 MW and DG2 presents a nominal power of 0.7 MW. In the microgrid, FES and BESS present droop controls to provide frequency support to the microgrid during the disturbance due to the islanding transition.

In the simulations, islanding occurs by the opening of Switch B located between bus 2 and the substation at 4s of simulation. After the islanding detection, the control of the synchronous generator, connected to bus 4, is changed to regulate the frequency and voltage of the microgrid. In this case, the frequency and voltage controls are performed by the synchronous generator and during disturbances the other sources will also provide temporary support.

In the control of the DFIG-based wind generator (DG2), two control loops are incorporated in the rotor side converter to provide temporary frequency support to the microgrid during the islanding transition. These control loops provide frequency support by releasing the kinetic inertia contained in the rotating masses as a function of the frequency deviation, considering a droop control, and as a function of rate of change of frequency (ROCOF), as presented in Fig. 4. In Fig. 4, (Δf) refers to the frequency deviation, in relation to the nominal frequency, (f_{nom}), and the frequency of the network (f), the (K_{Droop}), represents the gain of the droop control, and (K_{Rocof}) represents the gain of the ROCOF control. A signal coming from islanding detection scheme is responsible for activating the control, when the microgrid becomes islanded. During normal operation, when the microgrid is either grid-connected or islanded, the DFIG is controlled to

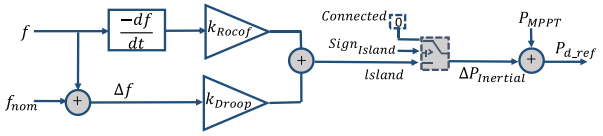

FIGURE 4. DFIG inertial control.

maximum power by the use of the Maximum Power Point Tracking Control-(MPPT).

Thus, the temporary frequency support provided by the DFIG is calculated by:

$$P_{d\_ref} = (P_{MPPT} - (K_{Drood}\,(f - f_{nom})) - \left(K_{Rocof}.f\,\frac{df}{dt}\right) \tag{10}$$

where, P_{MPPT} is the power delivered by the -(MPPT).

Fig. 5 presents the FES, which is composed by an induction machine coupled to a flywheel and connected to the grid by a voltage source converter (VSC) with a common DC link and an LCL filter. The converter control is responsible to keep the charge of the flywheel under steady state operation and, in an islanding event, it uses the kinetic energy stored in the flywheel to deliver power to the grid. When the measured frequency deviates from the nominal frequency, an error signal will be sent to PI controllers, generating a signal that changes the flywheel output power, providing the frequency regulation [54].

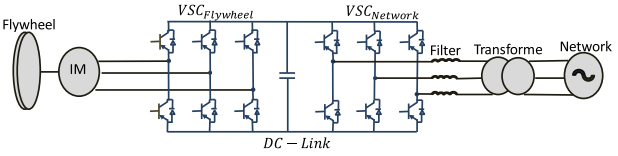

FIGURE 5. Flywheel energy storage.

The BESS consists of a generic model of a non-linear battery, connected to a voltage source inverter (VSI), as illustrated in Fig. 6 (b) [55]. The BEES has two control systems. The first one is related to its normal operation, which controls the charge/discharge in normal operation conditions. Different strategies can be used for this purpose, such as the ones presented in [56], [57]. In this paper, as the goal is to simulate the system dynamic response and assess the system response for different conditions, the SoC of the BESS is represented by a distribution function, limited to a percentage of ($20 < soc < 70$), which represents the limits SoC of the BESS operation [58]. The second control system implemented in the BESS provides temporary frequency support to the microgrid during disturbances, as islanding transition. In this case, the charge/discharge for normal operation will be interrupted and, if the BESS presents the minimum SoC, it will provide temporary frequency support using a droop control, as presented in Fig. 6 (a). This support is activated when the microgrid is islanded and the frequency variation

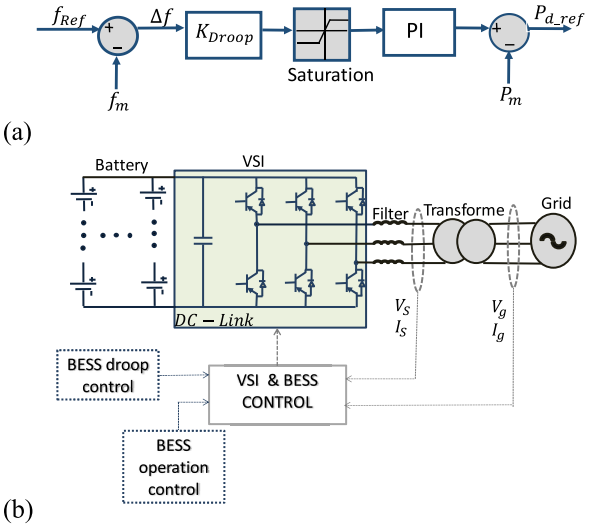

FIGURE 6. BESS droop control.

is higher than a bandwidth of 1 Hz, representing that the microgrid needs frequency support. During frequency support, if the battery is discharging and the SoC reaches the minimum limit, the power injection by the BESS will be interrupted and it will remain without exchanging power with the microgrid until the frequency is restored and the charging is enabled according to the algorithm for charge/discharge for islanding operation.

The microgrid is provided with a central controller, which is responsible for exchanging information among the elements and sending signals to change the controls of the DG units and storage systems. This control will collect and process measurements from the PCC voltage, Bus 2 in Fig. 3. After processing this information, if the islanding is detected, the central controller will send the signal to other elements of the microgrid to change their operation mode.

A hybrid islanding detection technique is used [59]. This technique employs voltage and frequency measurements, as a passive technique, associated with an active technique that causes a disturbance in the power of the DG to identify the operating condition of the network [59], the logic is presented in the flowchart of Fig. 7. The logic is implemented in the central controller, the voltage is measured at Bus 2, and according to the measurement, a signal is sent to DG1 to change its reference of output power to check if the microgrid is islanded. If the islanding operation is confirmed, the central controller sends a signal to all elements of the microgrid to change their control modes.

Initially, the voltage variations in the network are monitored $(\mathrm{dv}/\mathrm{dt})$, if they exist, the average voltage variation for five cycles ($\Delta \mathrm{v}_{\mathrm{mean},5}$) is calculated and compared to the accepted lower limit ($\Delta \mathrm{v}_{\mathrm{min}}$). If the lower limit is violated, it is checked if there is an island or if there is a disturbance of a different nature in the network. If ($\Delta \mathrm{v}_{\mathrm{mean},5}$) surpasses the higher limit ($\Delta \mathrm{v}_{\mathrm{max}}$), the detection algorithm indicates

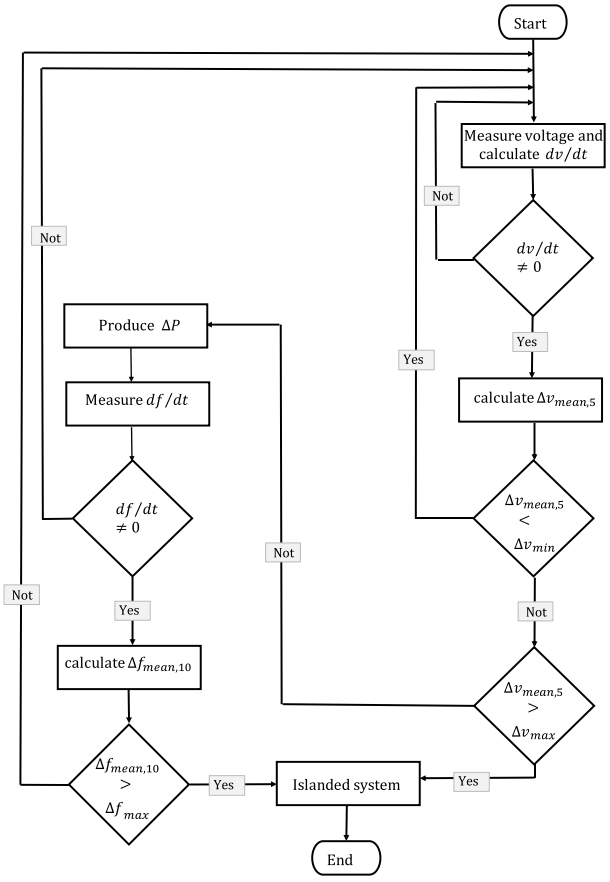

FIGURE 7. Flowchart of the islanding detection scheme.

the islanding condition. If ($\Delta \mathrm{v}_{\mathrm{mean},5}$) is found between the lower and maximum limits, a variation in the reference output power of the GD is caused. This variation is produced by means of a step, which must have a small amplitude, it is suggested in the range between 0.01 to 0.05 p.u, and duration of a few hundred milliseconds, between 200 to 600 ms. If the system is operating in islanded mode, the disturbance will cause the frequency change and islanding can be identified. This technique showed effectiveness to detect islanding condition with small detection time, which is a requirement for the islanding transition problem.

V. SIMULATION RESULTS

The simulations were performed using the software MatLab, using the test system illustrated in Fig. 3, which represents a microgrid connected to the utility distribution system. The islanding is simulated by the opening of the Switch B located between the bus 2 and the substation at 4s of simulation. The voltage at the PCC is monitored to check if the islanding transition is successful. For this purpose, two requirements are used. The first one is related to the protection. The IEEE Standard for Interconnection and Interoperability of Distributed Energy Resources with Associated Electric Power Systems Interfaces establishes the standard mandatory

frequency and voltage tripping requirements, presented in Table 1 and in Table 2, respectively [60]. These requirements are standard when no specific settings are required by the distribution system operator. Thus, once voltage or frequency reaches these limits, the generators are disconnected from the microgrid and the islanding transition is classified as not successful.

TABLE 1. Default settings for mandatory frequency tripping requirements.

Shall Trip Function	Frequency [Hz]	Clearing time [s]
OF2	62.0	0.16
OF1	61.2	300.0
UF1	58.5	300.0
UF2	56.5	0.16

TABLE 2. Default settings for mandatory voltage tripping requirements.

Shall Trip Function	Voltage [p.u.]	Clearing time [s]
OV2	1.20	0.16
OV1	1.10	2.0
UV1	0.70	2.0
UV2	0.45	0.16

Where, "OF" is over frequency and "UF" is under frequency in Hz.

Where, "OV" is over voltage and "UV" is under voltage in p.u.

Additionally, distribution grid codes related to power quality should also be considered. According to the Brazilian distribution grid code, in normal conditions, the frequency should be maintained in the range of 59.9 – 60.1 Hz. During disturbances at the distribution system, the frequency should return to the range of 59.5 – 60.5 Hz in 30s [61]. During this period, the frequency should stay in the range presented in Table 3. For voltage, the grid code presents the normal and critical voltage levels, which are presented in Table 4. Thus, as it is possible to verify, the trip requirements for Distributed Energy Resources are more restrictive than power quality constrains of grid code and will be used as the limits to identify successful islanding transition.

TABLE 3. Default settings for mandatory frequency tripping requirements.

Shall Trip Function	Frequency [Hz]	Maximum Allowed Time [s]
OF2	63.5	10
OF1	62	30
UF1	58.5	10
UF2	57.5	5

TABLE 4. Distribution grid code – voltage limits.

Classification	Voltage Range [p.u.]
Normal	$0.93 \leq V \leq 1.05$
Critical	$0.90 \leq V < 0.93$

Thus, using the methodology described in Section III, MCS are run to evaluate the probability of success islanding transition. Samples of load, wind, and status of charge of the battery, SoC, are generated. The wind distribution is represented by $v_m = 7.88$ m/s c=8.89 and k=2.The multivariate normal distribution was used to generate the battery charging samples and the Gaussian mix model with three components was used to model the load. The proportions of the distributions, primer component, second component and third component are presented in Tables 5, 6 e 7. Following the sequence, the hybrid technique was used for the islanding detection of the microgrid. The parameters used in the hybrid technique are: $\Delta V_{min} = 0.01 p.u; \Delta V_{max} = 0.5 p.u$; $\Delta f_{max} = 0.005\, p.u$; $\Delta f_{min} = 0.0001\, p.u$; $\Delta P = 0.05\, p.u$ per 500 ms.

TABLE 5. Gaussian mix model for the load.

Component 1	Component 2	Component 3
0.193	0.57	0.237

TABLE 6. Parameters of load gaussian mix model.

Component	Active Power [MW]	Reactive Power [MVAR]
1	2.8352	0.2891
2	1.3968	0.1794
3	1.5252	0.1981

TABLE 7. Covariance matrix of the first, second and third component.

Component	Active Power [MW]	Reactive Power [MVAR]
1	0.0170	0.0072
	0.0072	0.0031
2	0.0240	0.0122
	0.0122	0.0063
3	0.0286	0.0126
	0.0126	0.0057

During the grid-connected operation, it is assumed that the synchronous generators maintain a fixed power level injection into the grid. Usually, this power level is determined by its energy purchasing contract. Based on this assumption, the following first scenarios and configurations were considered:

- **Case 1**: DG1injecting 800 kW during the grid-connected operation, DG2 and FES connected to the microgrid.
- **Case 2**: DG1injecting 800 kW during the grid-connected operation, DG2 and BESS connected to the microgrid.

The result for Case 1 is presented in Table 8, and for Case 2, in Table 9. Different capacities of BESS and FES were simulated since their capacity of providing power during the islanding transition has a major impact on the successful of this transition.

As one can see in Table 8 and 9, the use of FESS can be more effective to improve the islanding transition, mainly because it can provide active power support during the islanding in any time, since the flywheel remains charged during grid-connected operation. On the other hand, SoC of BESS depends on its status at the instant of the islanding occurrence,

TABLE 8. Simulation results case 1.

DG1 injecting 800 kW			
Number of Simulations	Nominal Power FES	Probability of Success of the Islanding	Dispersion Coefficient
N	[kW]	E(x)	β
400	100	90.50%	1.62%
	200	96.50%	0.95 %
	300	99.50%	0.35%

TABLE 9. Simulation results case 2.

DG1 injecting 800 kW			
Number of Simulations	Nominal Power BESS	Probability of Success of the Islanding	Dispersion Coefficient
N	[kW]	E(x)	β
400	250	81.00 %	2.42 %
	300	91.75%	1.50%
	350	94.75%	1.17%

which is represented in the model by a distribution function. The BESS can be charging/discharging at the islanding occurrence. In the case it is charging, and the islanding is detected, the charging process will be interrupted and, if the BESS has enough energy stored, it will provide active power support to the grid. In these cases, it gives an important frequency support to the microgrid. In the case it is discharging at the instant of islanding occurrence, the power injected into the microgrid will be increased to its limit to support the frequency.

In Table 8 and 9, a high probability of successful islanding transition is obtained with the increase of the capacity of storage devices, as expected. For the load distribution considered for the base case, high levels of probability of successful transition were obtained for storage energy devices with capacity around 300 kW. It is important to highlight that the temporary support of the active power is important at the first seconds after the islanding and, after that, the frequency will be regulated by the synchronous generator-based DG, which usually depends on limited energy resource and remain connected to increase the system reliability, specially, during islanded operation mode.

It is important to highlight, from this simulated case, that a FES of 100kW is more effective than a BES of 250 kW for a successful islanding transition. A FES of 300 kW results in a 99.5 % rate of successful islanding transition, while a BESS of 350 kW results in only 94.75 % rate of successful islanding transition. Thus, when a successful transition to islanding operation is necessary, the increase in the BESS capacity may not be so effective as the use of FES. These numbers highlight the importance of the analysis of the security assessment of the islanding transition of microgrids.

The islanding transition is also evaluated for a higher power level injected in the grid, also considering different configurations and capacities, as following:

TABLE 10. Simulation results case 3.

DG1 injecting 1MW			
Number of Simulations	Nominal Power FES	Probability of Success of the Islanding	Dispersion Coefficient
N	[kW]	E(x)	β
400	100	97.50 %	0.80 %
	200	99.75 %	0.25 %
	300	100 %	0 %

TABLE 11. Simulation results case 4.

DG1 injecting 1MW			
Number of Simulations	Nominal Power BESS	Probability of Success of the Islanding	Dispersion Coefficient
N	[kW]	E(x)	β
400	250	94.50 %	1.20 %
	330	95.25%	1.11%

- **Case 3**: DG1 injecting 1.0 MW during the grid-connected operation, DG2 and FESs connected to the microgrid.
- **Case 4**: DG1 injecting 1.0 MW during the grid-connected operation, DG2 and a BESS connected to the microgrid.

As we can see in Table 10 and 11, the increase on the generation level of the synchronous generator improved the probability of a successful islanding transition. Considering the synchronous generator injecting 1 MW, a 97.5% probability of successful transition was obtained using a 100 kW FES, while for a 800-kW synchronous generator the probability using the same 100-kW FES was of 90.5%. Similar conclusions can be made by the configuration employing BESS. Based on the results presented, it is possible to assess the probability of a successful islanding transition considering specific coordinated control strategy without load shedding.

In order to consolidate the conclusions about the power injected by the synchronous-based DG, simulations decreasing the injected power by this DG are run, as following:

- **Case 5:** DG1 injecting 500 kW during the grid-connected operation, DG2 and FESs connected to the microgrid.
- **Case 6:** DG1 injecting 500 kW during the grid-connected operation, DG2 and a BESS connected to the microgrid.

The results for DG1 injecting 500 kW are presented in Table 11 and 12, for FES and BESS devices, respectively. As one can see, the overall probability of successful transition was reduced with the decrease of the power injected by the synchronous generator. This behavior is justified by the fact that with a higher power being injected, the microgrid is closed to the balance between load and generation and, therefore, it depends less on frequency support provided by other devices from the microgrid.

TABLE 12. Simulation results case 5.

DG1 injecting 500 kW			
Number of Simulations	Nominal Power FES	Probability of Success of the Islanding	Dispersion Coefficient
N	[kW]	E(x)	β
400	100	85.25%	2.08%
	200	90.25%	1.64%
	300	91.00%	1.57%

TABLE 13. Simulation results case 6.

DG1 injecting 500 kW			
Number of Simulations	Nominal Power BESS	Probability of Success of the Islanding	Dispersion Coefficient
N	[kW]	E(x)	β
400	250	76.75%	2.75%
	300	79.75%	2.52%
	350	80.00 %	2.50%

VI. DISCUSSION

The performance of the controls, used to improve the islanding transition, depends on the operation point during the islanding. Typically, these controls are tested for only few operating conditions, however, the possible operation points in a microgrid vary according to the availability of renewable resources, load level, and BES state of charge. These variables present a stochastic behavior and are typically characterized by density distribution functions. Thus, the proposed methodology allows evaluating the overall performance of the microgrid, considering all resources used to allow a successful islanding transition.

In the test system used in this paper, the following resources have been employed to improve the islanding transition performance:

- Synthetic inertia of the wind generator.
- Specific control for BESS during islanding transition.
- FES.

The use of stochastic simulation allows evaluating the overall effectivity of these resources for the islanding transition. The synthetic inertia can only contribute to frequency support when the operating point of the wind generator is under the nominal power and above the minimum rotor speed. In the case of the BESS, it can only provide frequency support if its SoC is above the minimum.

The main drawbacks of the proposed methodology are the number of simulations required and the need of modeling the behavior of some elements using density distribution functions. However, it is worth to emphasize that the required data is typically available for Distributed Energy Resources (DER) and, there are measurements available for computing these distribution functions. For example, usually measurements of wind speed are collected before the installation of the wind generators. Besides, considering a microgrid structure, load level can be easily monitored to compute the load distribution.

The procedure to evaluate the use of devices or specific controls to improve the islanding transition is mainly based on the available structure. The proposed methodology allows evaluating the overall effectiveness of each resource. Different techniques and/or devices can be used to improve the islanding transition, the effectivity of these devices can be tested by using the proposed methodology, presented in the flowchart of Figure 1. Thus, for projects that a specific successful rate of islanding transition is required, the following steps can be applied:

- **Step 1**: Apply the proposed methodology presented in flowchart of Figure 1. If the successful rate of islanding transition is under the required level, go to Step 2. Otherwise, the microgrid reached the required successful islanding rate.
- **Step 2**: Change the control, device, or device capacity of the elements that support the microgrid to islanding transition and go to Step 1.

VII. CONCLUSION

In this paper, a method for security assessment for the islanding transition of microgrids has been proposed. The method is based on Monte Carlo simulations, employing the probability distribution functions of intermittent generation and loads. As a result, the method allows calculating the probability of a successful islanding transition for a microgrid. The method is useful for evaluating the impact of different devices that can be used to minimize the probability of unsuccessful islanding transition. It is important to highlight that the transition to islanded operation due to an unintentional islanding without using load shedding is an important feature for microgrids, as the use of microgrids emerges as a solution to the increase connection of renewable energy to the grid and demand for enhancing the grid reliability.

In this context, the use of the proposed methodology enables evaluating different solutions to ensure the microgrid stability during these disturbances. It is important to highlight that the data required for this analysis can be easily obtained from monitoring devices usually employed for different purposes in a microgrid. In the case presented for validation, it was possible to verify that a FES can be more effective for islanding transition than a BESS due to the possibility that the BESS may not have enough energy stored at the instant of islanding. Thus, considering the proposed methodology, the effectiveness of different operating strategies or control techniques can be tested considering the whole possibility of operating points.

REFERENCES

[1] A. Dagar, P. Gupta, and V. Niranjan, "Microgrid protection: A comprehensive review," *Renew. Sustain. Energy Rev.*, vol. 149, Oct. 2021, Art. no. 111401, doi: 10.1016/j.rser.2021.111401.

[2] W. Chen and H. Yin, "Optimal subsidy in promoting distributed renewable energy generation based on policy benefit," *Clean Technol. Environ. Policy*, vol. 19, no. 1, pp. 225–233, Jan. 2017, doi: 10.1007/s10098-016-1216-x.

[3] J. D. Rios Penaloza, J. A. Adu, A. Borghetti, F. Napolitano, F. Tossani, and C. A. Nucci, "Influence of load dynamic response on the stability of microgrids during islanding transition," *Electr. Power Syst. Res.*, vol. 190, Jan. 2021, Art. no. 106607, doi: 10.1016/j.epsr.2020.106607.

[4] C. A. Cañizares, J. Reilly, and R. P. Behnke, "Microgrid stability definitions, analysis, and modeling," IEEE Power Energy Soc., Piscataway, NJ, USA, Tech. Rep. 113, 2018.

[5] K. H. Anderson, N. A. DiOrio, D. S. Cutler, and R. S. Butt, "Increasing resiliency through renewable energy microgrids," *Int. J. Energy Sector Manage.*, vol. 2, p. 17, Aug. 2017.

[6] A. A. Arefin, H. Masrur, M. L. Othman, H. Hizam, N. I. Abdul Wahab, N. A. Jalaluddin, and S. Z. Islam, "Power resilience enhancement of a PV- battery-diesel microgrid," in *Proc. Int. Conf. Smart Grids Energy Syst. (SGES)*, Nov. 2020, pp. 860–863, doi: 10.1109/SGES51519.2020.00158.

[7] O. A. Ansari, N. Safari, and C. Y. Chung, "Reliability assessment of microgrid with renewable generation and prioritized loads," in *Proc. IEEE Green Energy Syst. Conf. (IGSEC)*, Nov. 2016, pp. 1–6, doi: 10.1109/IGESC.2016.7790067.

[8] Y. Bian, Z. Bie, and Y. Lin, "A hierarchical optimization model for multi-microgrids to enhance power system resilience," in *Proc. IEEE Power Energy Soc. Gen. Meeting (PESGM)*, Aug. 2018, pp. 1–5, doi: 10.1109/PESGM.2018.8585932.

[9] K. Balasubramaniam, P. Saraf, R. Hadidi, and E. B. Makram, "Energy management system for enhanced resiliency of microgrids during islanded operation," *Electr. Power Syst. Res.*, vol. 137, pp. 133–141, Aug. 2016, doi: 10.1016/j.epsr.2016.04.006.

[10] A. Barnes, H. Nagarajan, E. Yamangil, R. Bent, and S. Backhaus, "Resilient design of large-scale distribution feeders with networked microgrids," *Electr. Power Syst. Res.*, vol. 171, pp. 150–157, Jun. 2019, doi: 10.1016/j.epsr.2019.02.012.

[11] Y. Chen, Z. Xu, and J. Østergaard, "Security assessment for intentional island operation in modern power system," *Electr. Power Syst. Res.*, vol. 81, no. 9, pp. 1849–1857, Sep. 2011, doi: 10.1016/j.epsr.2011.05.010.

[12] X. Tang, W. Deng, and Z. Qi, "Investigation of the dynamic stability of microgrid," *IEEE Trans. Power Syst.*, vol. 29, no. 2, pp. 698–706, Mar. 2014, doi: 10.1109/TPWRS.2013.2285585.

[13] S. Parhizi, H. Lotfi, A. Khodaei, and S. Bahramirad, "State-of-the-art research on micro grid stability: A review," *IEEE Access*, vol. 3, pp. 890–925, 2015, doi: 10.1080/01430750.2017.1412351.

[14] N. Soni, S. Doolla, and M. C. Chandorkar, "Improvement of transient response in microgrids using virtual inertia," *IEEE Trans. Power Del.*, vol. 28, no. 3, pp. 1830–1838, Jul. 2013, doi: 10.1109/TPWRD.2013.2264738.

[15] L. Rolim, M. Alves, T. M. L. Assis, P. O. L. Gatta, and G. N. Taranto, "Virtual inertia impact on microgrid voltage and frequency control," in *Proc. Simposio Brasileiro de Sistemas Eletricos (SBSE)*, May 2018, pp. 1–6, doi: 10.1109/SBSE.2018.8395661.

[16] K. Chen, "Stability of a community microgrid in islanded mode: A case study," in *Proc. 9th IEEE Int. Symp. Power Electron. Distrib. Gener. Syst. (PEDG)*, Jun. 2018, pp. 1–5, doi: 10.1109/PEDG.2018.8447735.

[17] F. C. L. Trindade, P. C. M. Meira, W. Freitas, and J. C. M. Vieira, "Control systems analysis of industrial plants with synchronous generators during islanded operation," in *Proc. IEEE PES Gen. Meeting*, Jul. 2010, pp. 1–8, doi: 10.1109/PES.2010.5589547.

[18] S. H. Hosseinian, B. Vahidi, and M. G. Rad, "Smart control mode selection for proper operation of synchronous distributed generators," in *Proc. Iranian Conf. Smart Grids*, May 2012, pp. 1–4.

[19] Y. Jingyan, H. Wei, Y. Renhua, Z. Jianhua, and Y. Xu, "Controlling and operating analysis of DFIG wind generator between in a large utility network and in an isolated micro-grid," in *Proc. IEEE Int. Conf. Sustain. Energy Technol.*, Nov. 2008, pp. 244–248, doi: 10.1109/ICSET.2008.4747010.

[20] O. Awedni, A. Masmoudi, and L. Krichen, "Power control of DFIG-based wind farm for system frequency support," in *Proc. 15th Int. Multi-Conf. Syst., Signals Devices (SSD)*, Mar. 2018, pp. 1298–1304, doi: 10.1109/SSD.2018.8570400.

[21] N. Sabpayakom and S. Sirisumrannukul, "Practical impact of VSPP in distribution networks: Intentional islanding operation," in *Proc. Australas. Universities Power Eng. Conf. (AUPEC)*, Sep. 2016, pp. 1–6.

[22] F. Katiraei, M. R. Iravani, and P. W. Lehn, "Micro-grid autonomous operation during and subsequent to islanding process," *IEEE Trans. Power Del.*, vol. 20, no. 1, pp. 248–257, Jan. 2005, doi: 10.1109/TPWRD.2004.835051.

[23] W. Al-Saedi, S. W. Lachowicz, D. Habibi, and O. Bass, "Power flow control in grid-connected microgrid operation using particle swarm optimization under variable load conditions," *Int. J. Electr. Power Energy Syst.*, vol. 49, no. 1, pp. 76–85, Jul. 2013, doi: 10.1016/j.ijepes.2012.12.017.

[24] C. Li, J. Savulak, and R. Reinmuller, "Unintentional islanding of distributed generation—Operating experiences from naturally occurred events," *IEEE Trans. Power Del.*, vol. 29, no. 1, pp. 269–274, Feb. 2014, doi: 10.1109/TPWRD.2013.2282264.

[25] P. Mahat, Z. Chen, and B. Bak-Jensen, "Review of islanding detection methods for distributed generation," in *Proc. 3rd Int. Conf. Electric Utility Deregulation Restructuring Power Technol.*, Apr. 2008, pp. 1–6, doi: 10.1109/DRPT.2008.4523877.

[26] S. C. Paiva, H. S. Sanca, F. B. Costa, and B. A. Souza, "Reviewing of anti-islanding protection," in *Proc. 11th IEEE/IAS Int. Conf. Ind. Appl.*, Dec. 2014, pp. 1–8, doi: 10.1109/INDUSCON.2014.7059454.

[27] R. S. Kunte and W. Gao, "Comparison and review of islanding detection techniques for distributed energy resources," in *Proc. 40th North Amer. Power Symp.*, Sep. 2008, pp. 1–8, doi: 10.1109/NAPS.2008.5307381.

[28] J. C. M. Vieira, D. Salles, and W. Freitas, "Power imbalance application region method for distributed synchronous generator anti-islanding protection design and evaluation," *Electr. Power Syst. Res.*, vol. 81, no. 10, pp. 1952–1960, Oct. 2011, doi: 10.1016/j.epsr.2011.06.009.

[29] W. Freitas, W. Xu, Z. Huang, and J. C. M. Vieira, "Characteristics of vector surge relays for distributed synchronous generator protection," *Electr. Power Syst. Res.*, vol. 77, no. 2, pp. 170–180, Feb. 2007, doi: 10.1016/j.epsr.2006.02.011.

[30] J. C. M. Vieira, W. Freitas, and D. Salles, "Characteristics of voltage relays for embedded synchronous generators protection," *IET Gener., Transmiss. Distrib.*, vol. 1, no. 3, pp. 484–491, May 2007, doi: 10.1049/iet-gtd:20060296.

[31] J. C. M. Vieira, W. Freitas, A. Morelato, and W. Xu, "Performance of frequency relays for distributed generation protection," *IEEE Trans. Power Del.*, vol. 21, no. 3, pp. 1120–1127, Jul. 2006, doi: 10.1109/TPWRD.2005.858751.

[32] J. C. M. Vieira, W. Freitas, W. Xu, and A. Morelato, "Efficient coordination of ROCOF and frequency relays for distributed generation protection by using the application region," *IEEE Trans. Power Del.*, vol. 21, no. 4, pp. 1878–1884, Oct. 2006, doi: 10.1109/TPWRD.2006.881588.

[33] N. B. Hartmann, R. C. dos Santos, A. P. Grilo, and J. C. M. Vieira, "Hardware implementation and real-time evaluation of an ANN-based algorithm for anti-islanding protection of distributed generators," *IEEE Trans. Ind. Electron.*, vol. 65, no. 6, pp. 5051–5059, Jun. 2018, doi: 10.1109/TIE.2017.2767524.

[34] S. Admasie, S. Basit Ali Bukhari, T. Gush, R. Haider, and C. Hwan Kim, "Intelligent islanding detection of multi-distributed generation using artificial neural network based on intrinsic mode function feature," *J. Mod. Power Syst. Clean Energy*, vol. 8, no. 3, pp. 511–520, 2020, doi: 10.35833/MPCE.2019.000255.

[35] A. Hussain, C. Kim, and S. Admasie, "An intelligent islanding detection of distribution networks with synchronous machine DG using ensemble learning and canonical methods," *IET Gener., Transmiss. Distrib.*, vol. 15, no. 23, pp. 3242–3255, Dec. 2021, doi: 10.1049/gtd2.12256.

[36] R. Haider, C. H. Kim, T. Ghanbari, and S. B. A. Bukhari, "Harmonic-signature-based islanding detection in grid-connected distributed generation systems using Kalman filter," *IET Renew. Power Gener.*, vol. 12, no. 15, pp. 1813–1822, Nov. 2018, doi: 10.1049/iet-rpg.2018.5381.

[37] S. Admasie, S. B. A. Bukhari, R. Haider, T. Gush, and C.-H. Kim, "A passive islanding detection scheme using variational mode decomposition-based mode singular entropy for integrated microgrids," *Electr. Power Syst. Res.*, vol. 177, Dec. 2019, Art. no. 105983, doi: 10.1016/j.epsr.2019.105983.

[38] P. Deshbhratar, R. Somalwar, and S. G. Kadwane, "Comparative analysis of islanding detection methods for multiple DG based system," in *Proc. Int. Conf. Electr., Electron., Optim. Techn. (ICEEOT)*, Mar. 2016, pp. 1525–1530, doi: 10.1109/ICEEOT.2016.7754939.

[39] L. Vinet and A. Zhedanov, "A 'missing' family of classical orthogonal polynomials," *Proc. IEEE*, vol. 105, no. 7, pp. 1311–1331, Nov. 2010, doi: 10.1088/1751-8113/44/8/085201.

[40] P. Mahat, Z. Chen, and B. Bak-Jensen, "A hybrid islanding detection technique using average rate of voltage change and real power shift," *IEEE Trans. Power Del.*, vol. 24, no. 2, pp. 764–771, Apr. 2009, doi: 10.1109/TPWRD.2009.2013376.

[41] R. R. Ferreira, P. J. Colorado, A. P. Grilo, J. C. Teixeira, and R. C. Santos, "Method for identification of grid operating conditions for adaptive overcurrent protection during intentional islanding operation," *Int. J. Electr. Power Energy Syst.*, vol. 105, pp. 632–641, Feb. 2019, doi: 10.1016/j.ijepes.2018.09.004.

[42] R. Y. Rubinstein and D. P. Kroese, *Simulation and the Monte Carlo Method*, 2nd ed. Hoboken, NJ, USA: Wiley, 2008.
[43] *Selected Statistical Methods for Analysis of Load Research Data*, Electr. Power Res. Inst., Washington, DC, USA, 1984.
[44] A. Seppala, "Statistical distribution of customer load profiles," in *Proc. Int. Conf. Energy Manage. Power Del. (EMPD)*, vol. 2, Nov. 1995, pp. 696–701, doi: 10.1109/EMPD.1995.500813.
[45] A. K. Ghosh, D. L. Lubkeman, M. J. Downey, and R. H. Jones, "Distribution circuit state estimation using a probabilistic approach," *IEEE Trans. Power Syst.*, vol. 12, no. 1, pp. 45–51, Feb. 1997, doi: 10.1109/59.574922.
[46] S. W. Heunis and R. Herman, "A probabilistic model for residential consumer loads," *IEEE Trans. Power Syst.*, vol. 17, no. 3, pp. 621–625, Aug. 2002, doi: 10.1109/TPWRS.2002.800901.
[47] G. W. Irwin, W. Monteith, and W. C. Beattie, "Statistical electricity demand modelling from consumer billing data," *IEE Proc. C (Gener., Transmiss. Distrib.)*, vol. 133, no. 6, p. 328, 1986, doi: 10.1049/ip-c.1986.0048.
[48] R. Herman and J. J. Kritzinger, "The statistical description of grouped domestic electrical load currents," *Electr. Power Syst. Res.*, vol. 27, no. 1, pp. 43–48, May 1993, doi: 10.1016/0378-7796(93)90058-M.
[49] A. Agostini and E. Celaya, "Reinforcement learning with a Gaussian mixture model," in *Proc. Int. Joint Conf. Neural Netw. (IJCNN)*, Jul. 2010, pp. 1–8, doi: 10.1109/IJCNN.2010.5596306.
[50] R. Singh, B. C. Pal, and R. A. Jabr, "Statistical representation of distribution system loads using Gaussian mixture model," *IEEE Trans. Power Syst.*, vol. 25, no. 1, pp. 29–37, Feb. 2010, doi: 10.1109/TPWRS.2009.2030271.
[51] O. A. Ansari, N. Safari, and C. Y. Chung, "Reliability assessment of microgrid with renewable generation and prioritized loads," in *Proc. IEEE Green Energy Syst. Conf. (IGSEC)*, Nov. 2016, pp. 1–6, doi: 10.1109/IGESC.2016.7790067.
[52] I. Segovia-Dominguez, A. Hernandez-Aguirre, and S. I. Valdez, "Designing the Boltzmann estimation of multivariate normal distribution: Issues, goals and solutions," in *Proc. IEEE Congr. Evol. Comput. (CEC)*, May 2015, pp. 2082–2089, doi: 10.1109/CEC.2015.7257141.
[53] J. E. Strapasson, J. Pinele, and S. I. R. Costa, "A totally geodesic submanifold of the multivariate normal distributions and bounds for the Fisher-rao distance," in *Proc. IEEE Inf. Theory Workshop (ITW)*, Sep. 2016, pp. 61–65, doi: 10.1109/ITW.2016.7606796.
[54] A. A. Khodadoost Arani, B. Zaker, and G. B. Gharehpetian, "Induction machine-based flywheel energy storage system modeling and control for frequency regulation after micro-grid islanding," *Int. Trans. Electr. Energy Syst.*, vol. 27, no. 9, p. e2356, Sep. 2017, doi: 10.1002/etep.2356.
[55] O. Tremblay, L.-A. Dessaint, and A.-I. Dekkiche, "A generic battery model for the dynamic simulation of hybrid electric vehicles," in *Proc. IEEE Vehicle Power Propuls. Conf.*, Sep. 2007, pp. 284–289, doi: 10.1109/VPPC.2007.4544139.
[56] M. A. Abdulgalil, M. Khalid, and F. Alismail, "Optimizing a distributed wind-storage system under critical uncertainties using benders decomposition," *IEEE Access*, vol. 7, pp. 77951–77963, 2019, doi: 10.1109/ACCESS.2019.2922619.
[57] A. Hussain, V.-H. Bui, and H.-M. Kim, "A proactive and survivability-constrained operation strategy for enhancing resilience of microgrids using energy storage system," *IEEE Access*, vol. 6, pp. 75495–75507, 2018, doi: 10.1109/ACCESS.2018.2883418.
[58] J. Tan and Y. Zhang, "Coordinated control strategy of a battery energy storage system to support a wind power plant providing multi-timescale frequency ancillary services," *IEEE Trans. Sustain. Energy*, vol. 8, no. 3, pp. 1140–1153, Jul. 2017, doi: 10.1109/TSTE.2017.2663334.
[59] P. J. Colorado, D. L. Silva, and A. P. Grilo, "Methodology for islanding operation of distributed synchronous generators," in *Proc. 19th Int. Conf. Intell. Syst. Appl. Power Syst. (ISAP)*, Sep. 2017, pp. 1–6, doi: 10.1109/ISAP.2017.8071366.
[60] IEEE Standards Coordinating Committee 21, *IEEE Standard Conformance Test Procedures for Equipment Interconnecting Distributed Energy Resources With Electric Power Systems and Associated Interfaces*, IEEE Stnadard 1547.1-2020, 2020.
[61] PRODIST. *Procedimentos de Distribuição de Energia Elétrica no Sistema Elétrico Nacional*. Accessed: Dec. 20, 2021. [Online]. Available: http://www.aneel.gov.br/modulo-8

PATRY J. COLORADO was born in Colombia. She is graduated in electrical engineering from the University Tecnológica of Pereira, Colombia, in 2012. She received the M.Sc. degree from the Federal University of ABC, in 2017. She is currently a Postgraduate Student of electrical engineering at the University of São Paulo (USP), Brazil. Her main research interests include distributed generation, stability and transition of microgrid operation with wind energy, and energy storage.

VINICIUS P. SUPPIONI was born in São Paulo, Brazil, in September 1982. He received the Bachelor of Science (B.Sc.) degree in electrical engineering from the Universidade Federal de Santa Catarina, Brazil, in 2007, and the Master of Science (M.Sc.) degree in energy engineering from the Universidade Federal do ABC, in 2011, where he is currently pursuing the Doctor of Philosophy (Ph.D.) degree in energy engineering. In 2017, he joined the Department of Electrical Engineering, Universidade Federal do ABC, as an Assistant Researcher. His research interests include renewable energy sources, wind generation, power quality aspects, and microgrids.

ALFEU J. SGUAREZI FILHO (Senior Member, IEEE) received the master's and Ph.D. degrees from Campinas University, Brazil, in 2007 and 2010, respectively. He is currently a Professor at the Federal University of ABC, Brazil, teaching in the areas of electrical machines, power electronics, and electrical drives. His research interests include machine drives, wind and photovoltaic energies, doubly-fed induction generators, power control, and electrical power systems.

MAURÍCIO B. C. SALLES (Member, IEEE) received the M.Sc. degree from the State University of Campinas (UNICAMP), São Paulo, Brazil, and the Ph.D. degree from the University of São Paulo (USP), in 2009. From 2006 to 2008, he joined the Research Team, Institute of Electrical Machines, RWTH Aachen University. He has been an Assistant Professor with the Polytechnic School, University of São Paulo, since 2010. From 2014 to 2015, he was a Visiting Scholar with the Harvard John A. Paulson School of Engineering and Applied Sciences. In 2018, he was an Invited Professor with the École Centrale de Lille, France. He is currently one of the founders of the Laboratory of Advanced Electric Grids—LGrid. His main research interests include distributed generation, power system dynamics, control and stability, renewable energy, energy storage, and electricity markets.

AHDA P. GRILO-PAVANI (Senior Member, IEEE) received the Ph.D. degree in electrical engineering from the University of Campinas, Campinas, Brazil, in 2008. She was a Visiting Scholar at the University of Alberta, Edmonton, Canada, in 2013. She is currently an Associate Professor at the Federal University of ABC—UFABC, Santo André, Brazil. Her main research interests include power system stability and control, integration of wind and PV power plants into power systems, and smart grids.